Progress In Electromagnetics Research Letters, Vol. 36, 21–30, 2013

THE SIMULATION AND EXPERIMENT OF A UWB PRINTED DIPOLE ANTENNA

Jia Lu, Shu Lin*, Yu Tian, Liwen Jing, Mengqian Liu, and Zhihua Zhao

School of Electronics and Information Engineering, Harbin Institute of Technology, 150080, P. R. China

Abstract—An ultra-wideband (UWB) printed antenna fed by balanced microstrip is proposed. This antenna is in the structure of symmetrical dipoles, each of which consists of 3 semicircular metal patches. The antenna has been simulated by CST MICROWAVE STUDIO® software and tested. Both the simulation and experimental results indicate that the proposed antenna obtains an ultra-wide bandwidth of 2.8–16.3 GHz, when VSWR is less than 2. The experimental results of the directional diagrams indicate that the proposed antenna acquires a balance feed within the whole working band. The analysis of the surface current on the radiators indicates that the proposed antenna has a radiation mode of standing wave current in low frequency and traveling wave current in high frequency. The length of the antenna on polarization direction is 0.315 times of the maximum working wavelength, which shows that the antenna is well miniaturized.

1. INTRODUCTION

With the rapid development of telecommunication technology, ultra wideband technology is attracting more and more attention. UWB antennas, as a vital part of the UWB telecommunication system, play an important role. Many literatures have proposed schemes for the design of UWB antennas, whose design philosophy can be summarized as follows: (1) Radiators in gradual changing structure has been proposed to achieve ultra-wide impedance bandwidth. This method is based on theory of small reflections (TSR). There are some typical antenna designs, such as the circular, the elliptic and the triangle

Received 19 September 2012, Accepted 7 November 2012, Scheduled 9 November 2012

* Corresponding author: Shu Lin (linshu@hit.edu.cn).

monopole antennas in reference [1–3], and the profiled monopole antennas in reference [4, 5]. (2) Antennas with loadings are proposed to achieve ultra-wide impedance bandwidth. Reference [6] proposed an antenna with loading on the feeding part, and Reference [7] presented a typical ultra-wideband antenna with loading on the radiator.

The proposed antenna realizes ultra-wide impedance bandwidth by integrating all the methods above. However, the radiation pattern bandwidth of the proposed antenna is narrower than the impedance bandwidth. In order to explain this phenomenon, the surface current on the radiators at a series of frequency points have been simulated and the amplitude and phase of the current have been extracted. Characteristics of the surface current on the radiator have been analyzed. The analysis explained the reason why the antenna radiation patterns rift at certain frequency region. Detailed simulation analysis and experimental results are shown in this paper.

2. ANTENNA MODEL AND SIMULATION RESULTS

The simulation model of the proposed antenna is shown in Fig. 1. The antenna is in a structure of double-side PCB. The material of this circuit board is FR4 epoxy plate whose relative dielectric constant $\varepsilon_r = 4.4$. The antenna is in a size of 46 mm × 36.2 mm with a thickness of 1.5 mm. The radiator of the antenna is composed of three semicircular patches. The radius of the semicircular patches are $R_1 = 14$ mm, $R_2 = 7$ mm and $R_3 = 3.5$ mm separately. This antenna is fed by balanced microstrip, and its radiators are symmetrical dipoles.

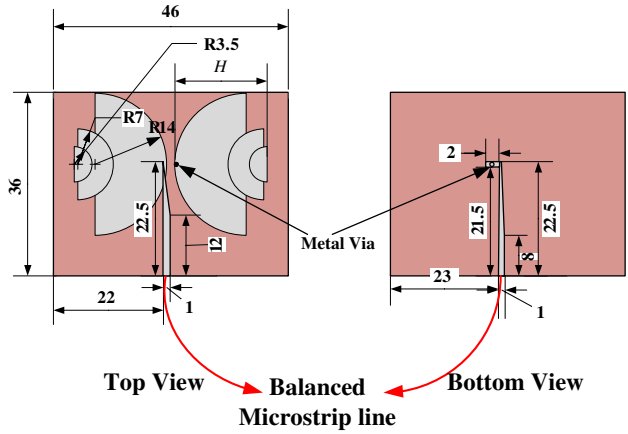

Figure 1. Printed antenna with semicircular combinatorial symmetrical radiators ($H = 18.1$ mm).

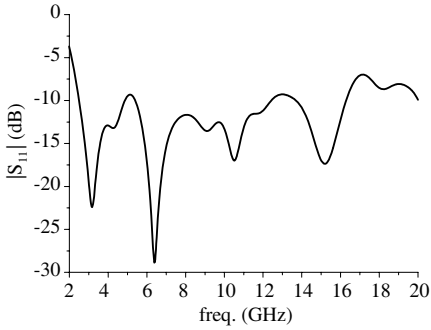

Figure 2. The simulation result of S-parameter.

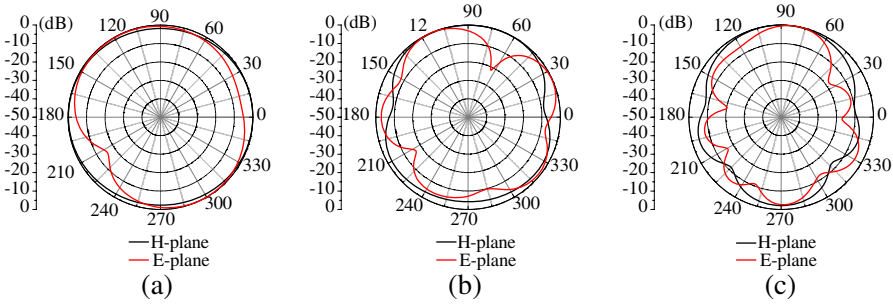

Figure 3. Radiation patterns of the printed antenna with combinatorial semicircular symmetrical dipoles. (a) 2.5 GHz, (b) 7 GHz, (c) 16 GHz.

The simulation result of the S-parameter is shown in Fig. 2. The working band is 2.5–16.3 GHz with $|S_{11}|$ less than -10 dB. The ratio bandwidth is over 6.5 : 1, which meets the requirement of UWB antennas. Furthermore, it is even wider than the FCC requirement for UWB antenna — 3.1–10.6 GHz (ratio bandwidth is 3.42 : 1).

The radiation patterns (in Fig. 3) indicate that the omni-directional radiation characteristics in H-plane begin to split and that the radiation pattern in E-plane does not show the typical shape "∞" when the frequency reaches 7 GHz or higher. This problem will be discussed in the analysis of simulated surface current below.

From the simulations of the proposed model, following conclusions can be drawn:

(1) The relationship between the initial operating frequency f and the height of the semicircular combinatorial symmetrical radiators H

is:

$$f_s\,(\mathrm{GHz}) = \frac{45}{H\ (\mathrm{mm})} \tag{1}$$

(2) For the semicircular combinatorial symmetrical radiators, the two small semicircular patches are equal to loads which can decrease the initial operating frequency.

(3) Compared with antennas in other literatures, the proposed antenna has relatively small size. Take the wafer UWB antenna in literature [8] for example. There is a relation between the initial operating frequency and the radiators' height: $f_s\,(\mathrm{GHz}) = \frac{55.6}{H\,(\mathrm{mm})}$. So this antenna is 20% bigger in size than the proposed antenna in this article.

3. SIMULATION RESULTS AND ANALYSIS OF THE SURFACE CURRENT

The proposed antenna was inspired by literature [4]. The antenna presented in [4] is a monopole antenna. The antenna's radiator is a semicircular metal patch which is fed by microstrip line, and the antenna ground is also a semicircular metal patch. This article designs a semicircular dipole antenna fed by microstrip line firstly, and then have its surface current simulated, as shown in Fig. 4(a). The simulated results show that the antenna surface current distributed mainly on the edge of the metal patch including the diameter of the semicircle in relatively low frequency (3 GHz). Since the current's resonance frequency is decided by the length of the current, the operating frequency of the antenna can be reduced by increasing the path length of antenna surface current. There are two ways to increase the path length: increasing the radium of the semicircle directly, and adding metal patches to the centre of the semicircle, as shown in Fig. 4(b). The reason for adopting the latter in this paper is that the dimension of the antenna radiators can be reduced, in order to realize the miniaturization the antenna.

The metal surface currents at some typical frequency points have been simulated, shown in Figs. 4(b)–(c). Simulation results indicate that current density is the biggest on edges of the radiators, which mainly determines the radiation field. While the surface currents on the two small semicircular patches are far smaller than that of the bigger ones, therefore, its influence can be ignored. Thus, as shown in Fig. 5, $i_1 \sim i_4$ primarily determine the radiation patterns.

At 2.5 GHz, we set the amplitude of i_3 as a comparison reference. Then we have $i_1 = 0.47$, $i_2 = 0.62$, $i_3 = 1$, $i_4 = 0.60$, $i_5 = 0.13$,

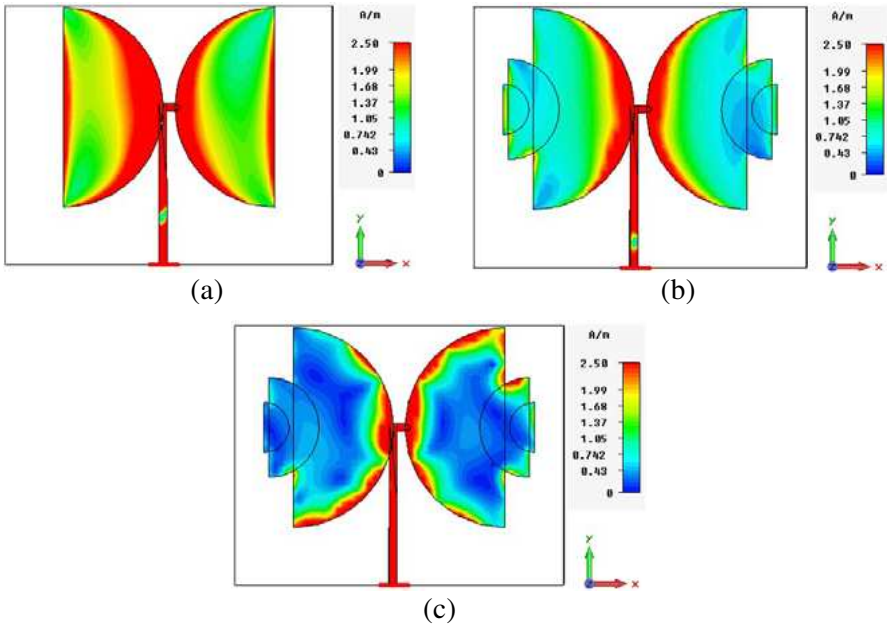

Figure 4. Simulation results of the metal surface current. (a) $f = 3.0\,\text{GHz}$, (b) $f = 2.5\,\text{GHz}$, (c) $f = 16\,\text{GHz}$.

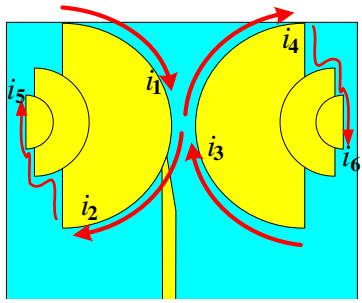

Figure 5. Edge currents on the antenna radiators.

$i_6 = 0.18$, which indicates that the currents primarily determine the radiation are $i_1 \sim i_4$.

3.1. Simulation Result of the Surface Current in Low Frequency Region

Figure 6 shows the amplitude and phase distribution of surface currents. Fig. 6 indicates that the phase variations among these four

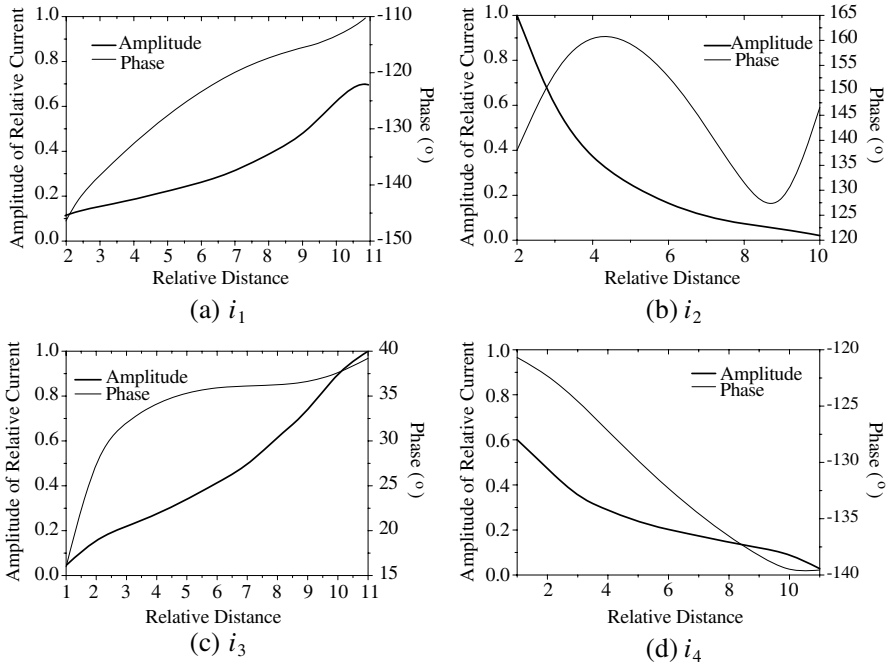

Figure 6. The amplitude and phase of edge currents on the radiators (2.5 GHz).

currents are all below 38.4° despite of the influence generated by the feeder line. The length of each current line, which is $\pi R_1/2 = 22$ mm, is equal to one fourth of the circumference. Such length can produce a space phase variation of 66° at 2.5 GHz (0.183 times of the wavelength). It can be seen that the real phase variation is smaller than the theoretical value. The maximum slow wave coefficient of the current wave is $\zeta = 0.582 < 1$. Thus, all four currents are standing wave currents at 2.5 GHz.

3.2. Simulation Results of the Surface Current in High Frequency Region

Figure 7 shows the current distribution of the amplitude and phase at 16 GHz. At 16 GHz, the phase variation of four currents are all over 422°. Such value is equal to the free space phase shift when the electromagnetic wave travels along one fourth of the circumference (1.173 times the wavelength). Thus, all four currents are traveling wave currents at 16 GHz.

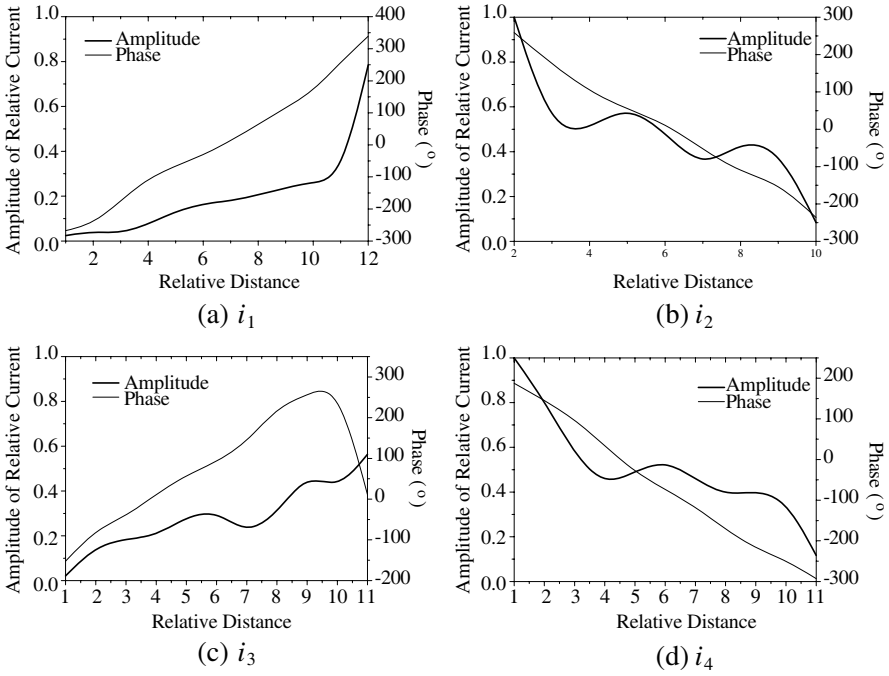

Figure 7. The amplitude and phase of the edge currents on radiators (16 GHz).

3.3. Analysis of the Simulation Results of Surface Current

The analysis results above indicate that the characteristics of metal surface current at low frequency region and at high frequency region are different. The current is standing wave current in low frequency region while it is traveling wave current in high frequency region. According to the theoretical analysis, when standing wave current has an electrical length shorter than the wavelength, the maximum radiation direction is perpendicular to the current direction. Meanwhile, it has omni-directional radiation characteristic in H-plane and low side-lobe level in E-plane. When the traveling wave current has an electrical length longer than the wavelength, the angle between the maximum radiation direction and the current direction is relatively small (less than 90°). So the plane perpendicular to the current direction has relatively low radiation. Meanwhile, the side-lobe level in E-plane is relatively high. Consequently, the radiation patterns begin to split up.

At 2.5 GHz in low frequency region, the length of the standing wave current line is 0.366 times of the wavelength. It can guarantee

the omni-directional radiation characteristic of the proposed antenna and the radiation patterns not splitting up. However, at 16 GHz in high frequency region, the traveling wave current line has a total length of 1.173 times of the wavelength. And splitting phenomenon occurs in the radiation patterns. Simulation results in Fig. 3 have also proved this. Therefore, if the wide radiation pattern bandwidth is required, miniaturization is necessary.

4. EXPERIMENTAL RESULTS

An antenna prototype is produced according to the designed antenna specifications, shown in Fig. 8. Measurements are carried out in a microwave anechoic chamber with Agilent E8363B Vector Network Analyzer. Test results are shown in Figs. 9–10. The experimental results are in close agreement with the simulation ones, which proves the correctness of both the simulation results and the analysis in Section 3.3. In addition, the measured $|S_{11}|$ bandwidth (2.8–20 GHz) is wider than the simulated bandwidth (2.5–16.3 GHz). It is caused

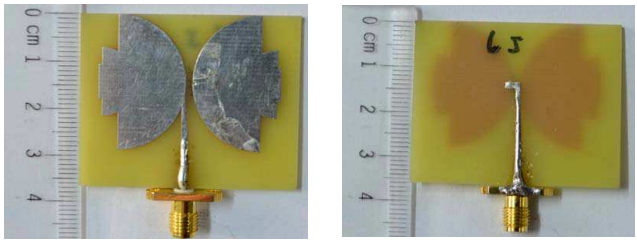

(a) Front (b) Back

Figure 8. Antenna prototype.

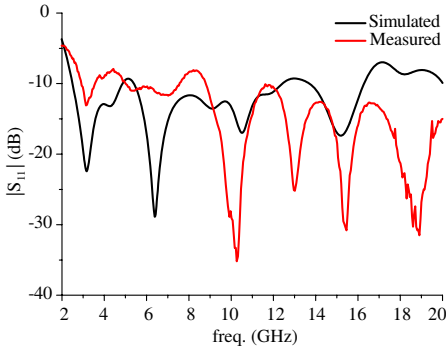

Figure 9. Tested $|S_{11}|$ of the antenna prototype.

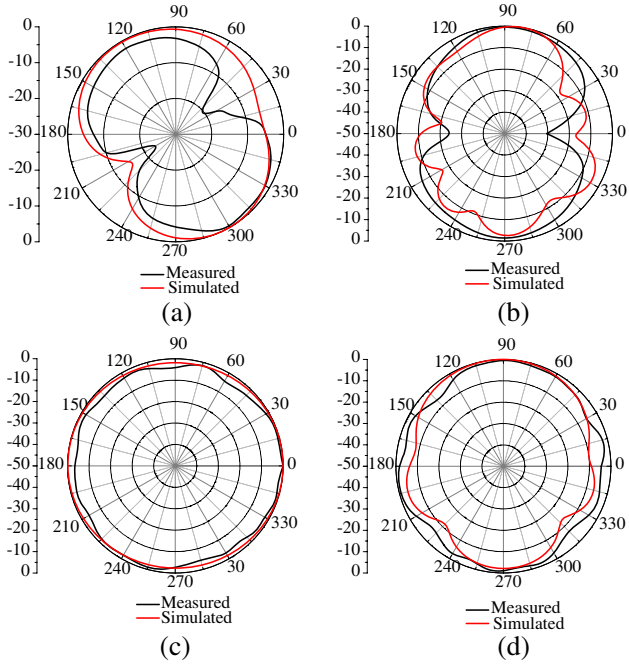

Figure 10. Tested results of the antenna. (a) Tested result of the antenna radiation pattern in E-plane (2.5 GHz). (b) Tested result of the antenna radiation pattern in E-plane (16 GHz). (c) Tested result of the antenna radiation pattern in H-plane (2.5 GHz). (d) Tested result of the antenna radiation pattern in H-plane (16 GHz).

by the use of FR-4 epoxy plate for the manufacture of the antenna prototype. It is a kind of loss material, and the loss will decrease the $|S_{11}|$ in high frequency region. Besides, the influence caused by dielectric slab and the fixture will cause little differences in the side lobes of the radiation patterns between experimental and simulation results.

5. CONCLUSION

A miniaturized UWB printed antenna with symmetrical dipoles is proposed. It has a working frequency range of 2.8–20 GHz (tested result). In the antenna design, an antenna unit with combinatorial semicircular symmetrical dipoles is proposed, which can improve the initial working frequency of $|S_{11}|$. By extracting the amplitude and phase of the surface current on the radiators, the current characteristics are analyzed. The analysis results indicate that traveling current

causes the splitting of the radiation pattern in high frequency region. Thus, when designing plane UWB omni-directional antennas, miniaturization is an effective way to reduce the difference between the radiation pattern bandwidth and the impedance bandwidth.

ACKNOWLEDGMENT

The authors would like to express their sincere gratitude to the financial support by the Fundamental Research Funds for the Central Universities (Grant No. HIT. NSRIF. 2010096).

The authors would also like to thank CST Ltd., Germany, for providing the CST Training Center (Northeast China Region) at our university with a free package of CST MWS software.

REFERENCES

1. Liang, J., L. Guo, and C. C. Chiau, "CPW-fed circular disc monopole antenna for UWB applications," *IEEE International Workshop on Antenna Technology*, 505–508, 2005.
2. Huang, C.-Y. and W.-C. Hsia, "Planar elliptical antenna for ultra-wideband communications," *Electronics Letters*, Vol. 41, No. 6, 296–297, 2005.
3. Lin, S., W. Wang, and Y. Liu, "Planar composite triangle monopole UWB antenna," *Proceedings of 2011 IEEE International Conference on Ultra-wideband (ICUW2010)*, Vol. 1, 1–3, 2010.
4. Bialkowski, M. E. and A. M. Abbosh, "Design of UWB planar antenna with improved cut-off at the out-of-band frequencies," *Antennas and Wireless Propagation Letters*, Vol. 7, 408–410, 2008.
5. Lizzi, L., G. Oliveri, and A. Massa, "A time-domain approach to the synthesis of UWB antenna systems," *Progress In Electromagnetics Research*, Vol. 122, 557–575, 2012.
6. Wu, Q., R. Jin, and J. Geng, "Printed ommi-directional UWB monopole antenna with very compact size," *IEEE Transactions on Antenna and Propagation*, Vol. 56, No. 3, 896–899, Mar. 2008.
7. Bai, X.-F., S.-S. Zhong, and X.-L. Liang, "Leaf-shaped monopole antenna with extremely wide bandwidth," *Microwave and Optical Technology Letters*, Vol. 48, No. 7, 1247–1250, 2006.
8. Liang, J., C. C. Chiau, X. Chen, and C. G. Parini, "Printed circular disc monopole antenna for ultra-wideband applications," *Electronics Letters*, Vol. 40, No. 20, 1246–1247, 2004.